Solid State Communications 242 (2016) 30–35

Contents lists available at ScienceDirect

Solid State Communications

journal homepage: www.elsevier.com/locate/ssc

Highlight

Phase transformation and fluorescent enhancement of ErF_3 at high pressure

Wentao Li [a,b], Xiangting Ren [b], Yanwei Huang [b], Zhenhai Yu [b], Zhongying Mi [b], Nobumichi Tamura [c], Xiaodong Li [d], Fang Peng [a,*], Lin Wang [b,e,f,**]

[a] Institute of Atomic and Molecular Physics, Sichuan University, Chengdu 610065, China
[b] Center for High Pressure Science and Technology Advanced Research (HPSTAR), Shanghai 201203, China
[c] Advanced Light Source (ALS), Lawrence Berkeley National Laboratory, Berkeley, CA 94720, United States
[d] Institute of High Energy Physics, Chinese Academy of Sciences, Beijing 100049, China
[e] State Key Laboratory of Superhard Materials, Jilin University, Changchun 130012, China
[f] High Pressure Synergetic Consortium, Geophysical Laboratory, Carnegie Institution of Washington, Argonne, IL 60439, United States

HPSTAR 2016-208

ARTICLE INFO

Article history:
Received 24 March 2016
Received in revised form
23 May 2016
Accepted 24 May 2016
Available online 26 May 2016

Keywords:
A. Rare-earth trifluorides
C. Structure and fluorescence
D. Phase transitions and enhancement of fluorescence
E. High pressure

ABSTRACT

Pressure-induced phase transformation and fluorescent properties of ErF_3 were investigated here using *in-situ* synchrotron X-ray diffraction and photoluminescence up to 32.1 GPa at room temperature. Results showed that ErF_3 underwent a reversible pressure-induced phase transition from the β-YF_3–type to the fluocerite LaF_3-type at 9.8 GPa. The bulk moduli B_0 for low- and high-pressure phases were determined to be 130 and 208 GPa, respectively. Photoluminescencent studies showed that new emission lines belonging to the transition of $^2H_{11/2} \rightarrow {}^4I_{15/2}$, $^4S_{3/2} \rightarrow {}^4I_{15/2}$, and $^4F_{9/2} \rightarrow {}^4I_{15/2}$ appeared during phase transition, suggesting pressure-induced electronic band splitting. Remarkably, significant pressure-induced enhancement of photoluminescence was observed, which was attributed to lattice distortion of the material under high pressure.

1. Introduction

The rare-earth trifluorides (REF_3) are important functional materials that have been widely used in laser sources, detectors, optoelectronics, and biological applications [1, 2–4] because of their unique physical and chemical properties, such as low phonon energy, high ionicity, high resistivity, and high anionic conductivity [5]. The phase stability and transformations of this family have received considerable attention because their properties are heavily dependent on their structures. It is known that REF_3 family has two crystal structures depending on the atomic size of the rare-earth element at ambient pressure and room temperature. For low-Z rare-earth elements from La to Nd, REF_3 crystallizes in the trigonal structure (tysonite-type, No. 165) with space group *P*-3*c*1. For other elements in the family, REF_3 has the orthorhombic structure (β-YF_3-type, No. 62) with space group *Pnma* [6,7]. Pressure, one of the most significant thermodynamic parameters, can change the interatomic distance directly, and therefore effectively tune the interactions among atoms, the structures and properties of materials. Pressure-induced phase transformations of the tysonite-type REF_3 has been focused on LaF_3 [9–13] and CeF_3 [14]. Using high pressure diffraction, Dyuzheva et al. observed the transition from tysonite-structure to *C*-centered orthorhombic (*Cmma* No. 67) structure in LaF_3 [8] and CeF_3 [14] at 19 and 20.6 GPa, respectively. Winkler et al. [10] calculated the high pressure phase of LaF_3, but proposed a tetragonal structure with *I*4/*mmm* symmetry which is different from that observed by Dyuzheva et al. Crichton et al. [9] examined the behavior of LaF_3 at high pressure by XRD and Raman spectroscopy and atomistic model calculations. They identified that the high pressure phase of LaF_3 is the anti-Cu_3Ti-type (*Pmmm*, No. 59), which is evidently similar to the *Cmma* symmetry reported by Dyuzheva et al., has been well accepted. For the β-YF_3-type REF_3, YF_3 [15] and EuF_3 [16] have been reported to have similar phase transformation from original orthorhombic phase to trigonal hexagonal phase. In summary, the phase transition sequence of REF_3 would be α-$UO_3 \rightarrow$ β-$YF_3 \rightarrow$ tysonite $\rightarrow$ anti-Cu_3Ti-type with increasing pressure, as observed experimentally up to date.

ErF_3 is one of the most important rare-earth trifluorides due to its sharp luminescence of Er^{3+} from the transitions among the intra-4*f* shell, the first excited state and the ground state of the ion. It has tremendous applications ranging from optoelectronics to

* Corresponding author.
** Corresponding author at: Center for High Pressure Science and Technology Advanced Research (HPSTAR), Shanghai 201203, China
E-mail addresses: pengfang@scu.edu.cn (F. Peng), wanglin@hpstar.ac.cn (L. Wang).

http://dx.doi.org/10.1016/j.ssc.2016.05.014
0038-1098/

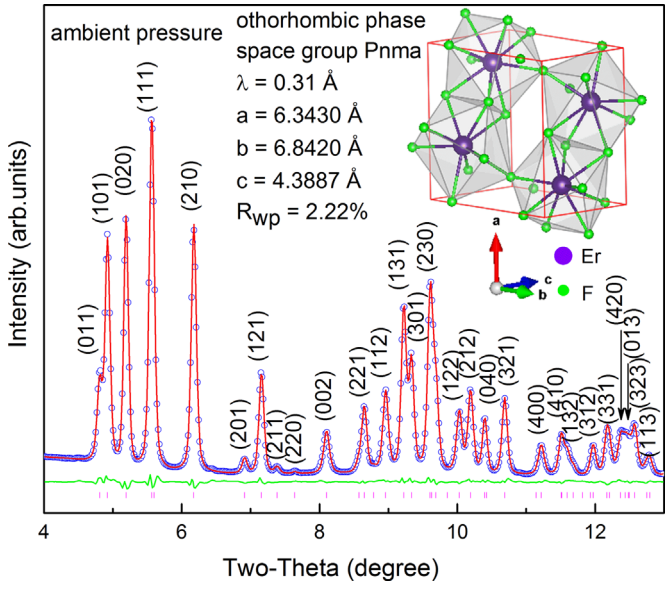

Fig. 1. The XRD pattern of ErF_3 under ambient conditions. The inset is the schematic crystal structure of ErF_3.

fiber communications [17,18]. The phase stability of ErF_3 directly affects its applications but no results on the structural stability of ErF_3 have been reported. Furthermore, exploring the phase evaluation in ErF_3 can provide insights into the relationship between their crystal structures and properties, and may also discover new properties.

In this work, the structural phase transition of ErF_3 was investigated using AD-XRD and photoluminescence (PL) measurement under high pressure up to 32.1 GPa. The XRD and PL studies showed that ErF_3 experiences a phase transition from the orthorhombic phase to trigonal phase at 9.8 GPa. Significant pressure-induced enhancement of fluorescence was observed before the phase transition. This might be due to the lattice distortion of the material at high pressure.

2. Experimental details

ErF_3 powder with a purity of 99.99% was purchased from Aladdin Industrial Corporation and used without further purification. A symmetrical type diamond anvil cell (DAC) with 300 μm diameter culet was used to generate high pressure. The sample was loaded into a 120 μm diameter hole drilled in a T301 stainless steel gasket, which was pre-indented to a thickness of 45 μm. Methanol-ethanol (4:1 by volume) was used as the pressure-transmitting medium and the pressure was determined from the ruby R1-luminescence line shift [19].

In-situ high pressure AD-XRD measurements were performed at the 4W2 beamline of Beijing Synchrotron Radiation Facility (BSRF, China) at room temperature with a wavelength of 0.6199 Å. A Si (111) monochromator was used to produce the X-ray beam. The incident X-ray beam was focused down to 21×8 μm using a pair of Kirkpatrick-Baez mirrors. The image-plate area detector (Mar345) was used to collect diffraction data and high-purity CeO_2 powder was used to calibrate the geometric parameters. FIT2D software was used to integrate the diffraction rings into one-dimensional patterns [20]. *In-situ* high-pressure fluorescence spectroscopic experiments of ErF_3 were measured using a He/Ne-mixed ion laser with wavelength of 532 nm to cover a wavelength range of 533–680 nm.

3. Results and discussion

Fig. 1 shows the AD-XRD of ErF_3 at ambient pressure. It can be indexed into the orthorhombic structure with space group *Pnma*, which is consistent with previous reports [21]. The inset schematic of crystal structure clearly shows that Er atoms are surrounded by nine F atoms. The selected pressure evolution of the AD-XRD patterns of ErF_3 for compression and decompression procedures are shown in Fig. 2a. With increasing pressure no change was observed up to 8.1 GPa, indicating that the sample remained in the orthorhombic phase. Upon further compression, a new peak appeared at around 12° as the pressure reached 9.8 GPa. New peaks appeared more intense while the peaks belonging to the orthorhombic structure started to disappear, indicating the onset of a phase transition. At 18.2 GPa all the diffraction peaks from the orthorhombic phase disappeared, and the only signal detected was that of the high-pressure phase, suggesting that the phase transition had been completed. This structure of the high-pressure phase of ErF_3 was new for ErF_3. By using the XRD analytical software MDI Jade, we found that the indexing of *P*-3*c*1 space group matches our AD-XRD the best. The high-pressure phase of ErF_3 is isostrucutral with the fluocerite-type LaF_3. The determination of high-pressure phase of ErF_3 in this work is consistent with the above mentioned isocompounds under high pressure reported in the literature [16]. In the light of the structural evolution of isocompouds under high pressure, we successfully refined the diffraction pattern of ErF_3 at 19.6 GPa using General Structure Analysis System (GSAS) [22,23]. The fitting result and refined parameters are shown in Fig. 2b and Table 1. The phase transition route was similar to that observed in EuF_3 [16]. As compression continued, no phase transition was found for the new phase up to 30 GPa, the highest pressure in the study. Upon decompression to ambient pressure, results showed that the trigonal structure had returned to an orthorhombic state, showing that the pressure-induced phase transition of ErF_3 is reversible.

Previous theoretical and experimental investigations suggested that short F–F distance leads to the pressure-induced structural phase transition in low-Z rare-earth trifluorides such as LaF_3, CeF_3 [12]. We have also investigated the F–F and Er–F bondings from our Rietveld analyses, as shown in Figs. 2d and 5c. It is clear that F–F and Er–F bondings both showed strong anisotropic compression behavior. Therefore, we speculated that the pressure-induced structural phase transition of ErF_3 was due to the remarkable anisotropic compression behavior in F–F and Er–F bondings.

The pressure dependence of the unit cell volume is shown in Fig. 2c. The pressure-volume data has been fitted to the third-order Birch–Murnaghan equation of state, as follows [24,25]:

$$P = \frac{3}{2}B_0\left[\left(\frac{V}{V_0}\right)^{\frac{-7}{3}} - \left(\frac{V}{V_0}\right)^{\frac{-5}{3}}\right] \times \left\{1 - 0.75\left(4 - B_0'\right)\left[\left(\frac{V}{V_0}\right)^{\frac{-2}{3}} - 1\right]\right\}$$

here B_0 and V_0 are bulk modulus and the volume under ambient conditions, respectively, and B_0' is the pressure derivative of B_0. The bulk modulus of the orthorhombic and trigonal phases was found to be at 130 (6) GPa and 208 (21) GPa, respectively, when B_0' was fixed at 4 in these two fittings. In previous work, the bulk modulus of LaF_3 CeF_3 and GdF_3 is 160.5 (2.7) GPa [9], 147 (10) GPa [14]and 132 (12) GPa [26]. It is interesting to note that the bulk moduli of REF_3 decrease as the ionic radii decrease.

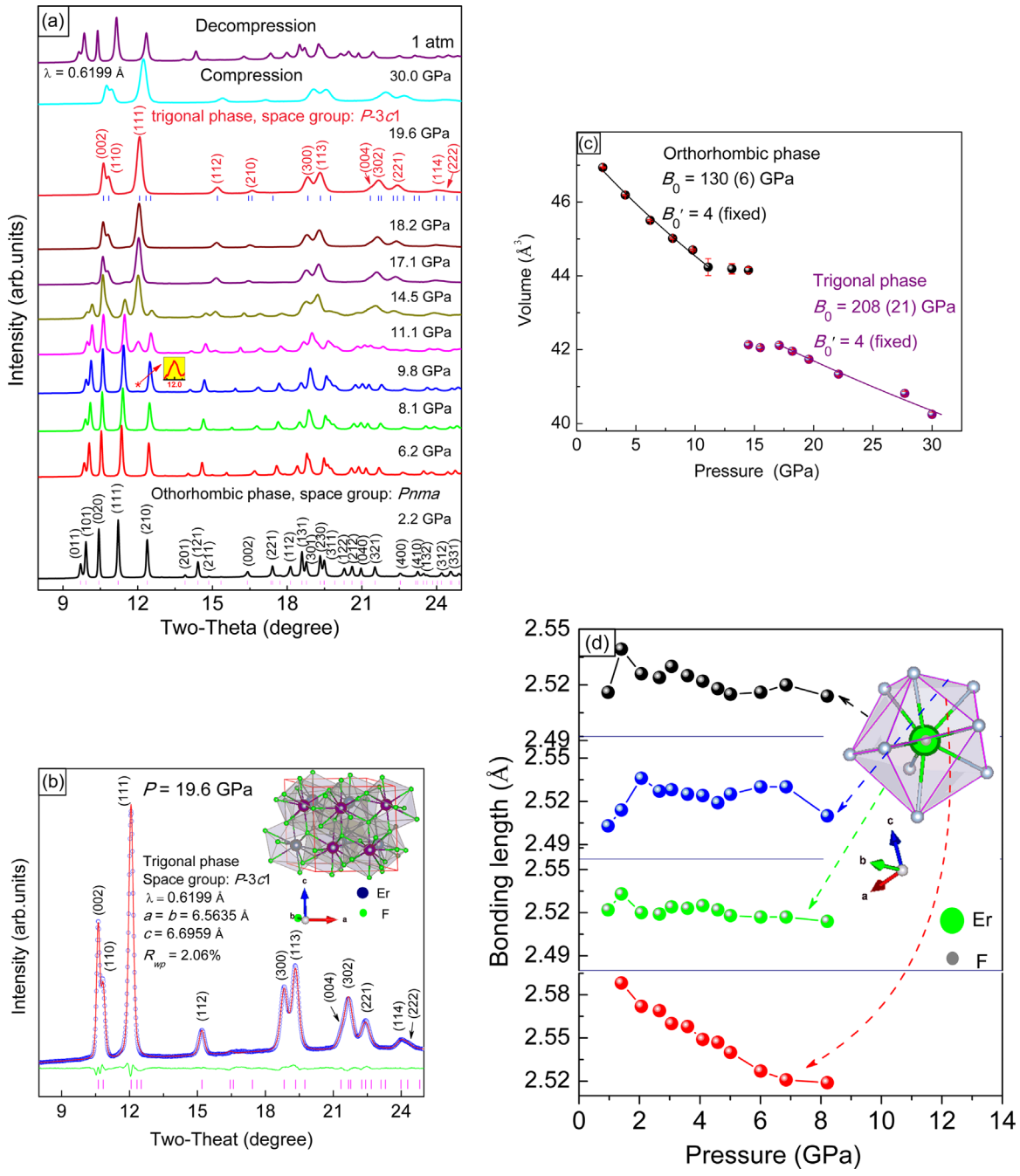

Fig. 2. (a) The selected AD-XRD of ErF_3 under high pressure during compression and decompression; (b) GSAS refinement of the diffraction pattern of ErF_3 at 19.6 GPa, insert is the schematic crystal structure of a high pressure phase of ErF_3; (c) Equation of state of the phases of ErF_3 and (d) Pressure dependences of the length of F–F bonding of ErF_3.

Table 1
Final refined parameters and values obtained at 19.6 GPa.

Cell			
a		6.5635(2) Å	
b		6.5635(2) Å	
c		6.6959(2) Å	
Space group		*P*-3*c*1	
Atom	*x*	*y*	*z*
Er	0.6662(1)	0	1/4
F(1)	0.3634(6)	0.0414(8)	0.0739(9)
F(2)	1/3	2/3	0.1730(5)
F(3)	0	0	1/4

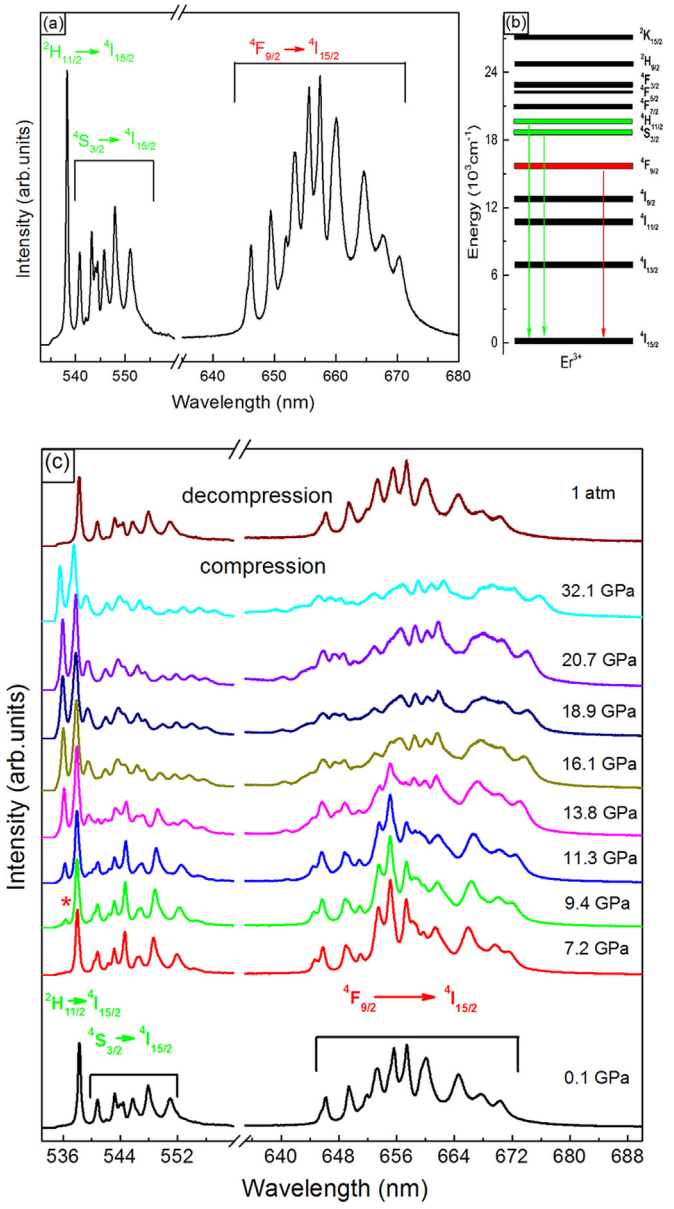

Fig. 3. (a) Photoluminescence spectra of ErF_3 with the 532 nm excitation laser under ambient pressure; (b) Simplified energy-level diagram of Er^{3+} and (c) Fluorescence spectrum of ErF_3 recorded with the 532 nm excitation laser under different pressures.

To investigate the influences of structural transition on the fluorescence properties of ErF_3, fluorescence was measured from ambient pressure up to 32.1 GPa. The fluorescence spectrum of ErF_3 at ambient pressure is shown in Fig. 3a. The green spectra (which ranged from 535 to 538 nm and from 540 to 552 nm) and the red spectrum (which ranged from 645 to 672 nm) were attributed to the transitions from Er^{3+} ion excited state levels $^2H_{11/2}$, $^4S_{3/2}$, and $^4F_{9/2}$, to the ground state level $^4I_{15/2}$ respectively [27, 28,29], as shown in the schematic in Fig. 3b.

Representative fluorescence spectra measured from 0.1 to 32.1 GPa are shown in Fig. 3c. Initially, the spectrum is the fluorescence signals of an orthorhombic phase. With increasing pressure, the spectra have no obvious changes except peak shifts up to 7.2 GPa, indicating that the structure remained stable up to this pressure, which was consistent with XRD results. As the pressure reached 9.4 GPa, a new peak appeared near 536 nm which can be assigned to the transition of $^2H_{11/2}\rightarrow{}^4I_{15/2}$. Upon further compression, two more groups of new peaks gradually appeared around 539–555 nm and 647–659 nm. These were attributed to the transitions of $^4S_{3/2}\rightarrow{}^4I_{15/2}$ and $^4F_{9/2}\rightarrow{}^4I_{15/2}$, respectively. However, as the pressure continued to increase above 18.9 GPa the fluorescence spectra of ErF_3 showed no obvious transformation. The pressure dependence of emission peaks is shown in Fig. 4. Results showed that the emission lines of $^2H_{11/2}\rightarrow{}^4I_{15/2}$ transition shifted to high energy monotonically as pressure increased. The emission lines of $^4S_{3/2}\rightarrow{}^4I_{15/2}$ and $^4F_{9/2}\rightarrow{}^4I_{15/2}$ responded to pressure very differently, but all showed discontinuity at the same pressure range. All of the above mentioned behaviors of luminescence spectra under increasing pressure suggested that the material may undergo a phase transition within the pressure range of 9.4–16.1 GPa, which corresponds to the results of XRD.

Interestingly, a remarkable enhancement of fluorescence from ErF_3 was observed at low pressures as shown in Fig. 5a. With increasing pressure the fluorescence intensity reached an experimental maximum at a pressure of 5.3 GPa. The maximum luminescence intensity was about 2 times of that at ambient pressure, as shown in Fig. 5b. According to the works of pioneering contributors [30-32] fluorescence intensity is determined by the radiative rates of the involved electronic transitions, reduction of the intermolecular distance, and localization of the density of Er^{3+} ions; which renders fluorescence more efficient with increasing pressure. Intermolecular distance was analyzed under a low-pressure regime as shown in Fig. 5c. Results showed that the pressure dependences in the interatomic distances of ErF_3 all showed anomalies under the same pressure regime, according to the intensity of luminescence. This suggests that the observed increase in fluorescence is attributable to changes in intermolecular interaction, caused by pressure-induced distortion. As reported by Wisser et al. [30], lattice distortion can cause beneficial Laporte selection rule relaxation, and the subsequent enhancement of fluorescence. Further compression produces a sharp reduction in fluorescence efficiency, which is probably caused by defect formation and phase transformation at higher pressures.

4. Conclusions

In summary, this study of the pressure-induced phase transition and PL properties of ErF_3 demonstrates that ErF_3 transformed from the β-YF_3–type to the fluocerite LaF_3-type structure at 9.8 GPa and remained stable up to 30 GPa. Upon decompression, the trigonal phase transformed back to the ambient pressure phase, suggesting that the transition is reversible. The bulk moduli of ErF_3 for both phases were determined as 130 (6) GPa and 208 (21) GPa. The *in-situ* high-pressure fluorescence was also measured at room temperature up to 32.1 GPa. New emission lines started to appear at 9.4 GPa, which indicates the occurrence of a pressure-induced structure transition of ErF_3, which corresponds with the high-pressure XRD results closely. Significant enhancement of fluorescence was observed under low pressure due to lattice distortion.

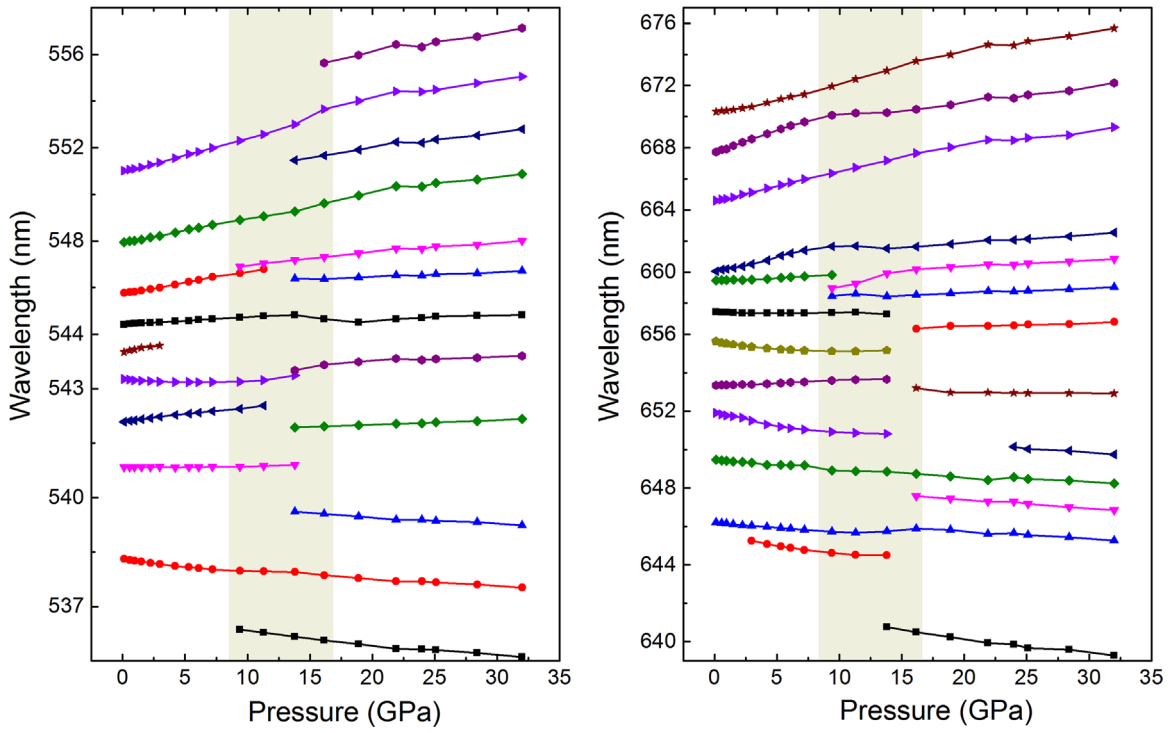

Fig. 4. Pressure-induced shifts of the luminescence peaks of ErF_3. The remarkable variation of emission lines under high pressure was marked with gray rectangular region. These results were consistent with the present XRD data.

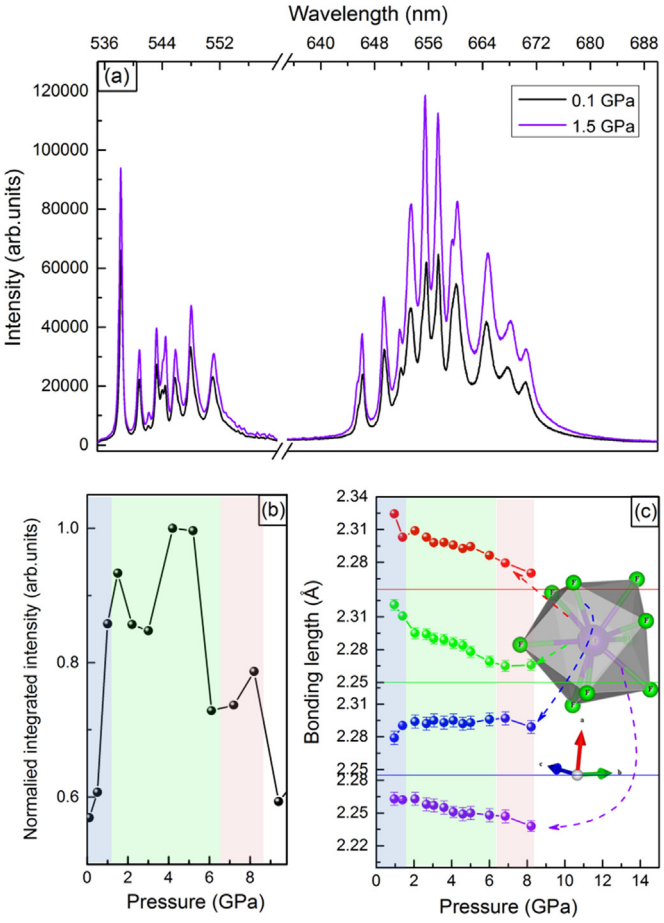

Fig. 5. (a) Comparison of fluorescence intensity at 0.1 GPa and 1.5 GPa. (b) Fluorescence intensity as a function of applied pressure and (c) Pressure dependences of the length of Er–F bonding of ErF_3.

Acknowledgments

This work was supported by the joint fund of the National Natural Science Foundation of China, China Chinese Academy of Sciences Fund (Grant no. U1332104) and NSAF (Grant no. U1530402). The high pressure XRD experiments were carried out at beamline 4W2 of the Beijing Synchrotron Radiation Facility (BSRF), which is supported by the Chinese Academy of Sciences (Grant no. KJCX2-SW-N03, KJCX2-SW-N20).

References

[1] L.Y. Wang, P. Li, Y.D. Li, Adv. Mater. 19 (2007) 3304.
[2] J.W. Stouwdam, F.C.J.M.V. Veggel, Nano Lett. 2 (2002) 733.
[3] D. Nagel, Laser Surg. Med. 21 (1997) 79.
[4] S. Jovanovic, D. Anft, U. SchÖnfeld, A. Serghaus, H. Scherer, Eur. Arch. Oto-Rhino-Laryngol 252 (1995) 422.
[5] C.G. Olson, M. Piacentini, D.W. Lynch, Phys. Rev. B 18 (1978) 5740.
[6] A. Zalkin, D.H. Templeton, J. Am. Chem. Soc. 75 (1953) 2453.
[7] A. Zalkin, D.H. Templeton, T.E. Hopkins, Inorg. Chem. 5 (1966) 1466.
[8] T.I. Dyuzheva, L.M. Lityagina, G.B. Demishev, N.A. Bendeliani, J. Alloys Compd. 335 (2002) 59.
[9] W.A. Crichton, P. Bouvier, B. Winkler, A. Grzechnik, Dalton Trans. 39 (2010) 4302.
[10] B. Winkler, K. Knorr, V. Milman, J. Alloys Compd. 349 (2003) 111.
[11] E.M. Diniz, C.W.A. Paschoal, Solid State Commun. 136 (2005) 538.
[12] E.M. Diniz, C.W.A. Paschoal, Phys. B 391 (2007) 228.
[13] P. Modak, A.K. Verma, S. Ghosh, G.P. Das, J. Phys. Chem. Solids 70 (2009) 922.
[14] T.I. Dyuzheva, L.M. Lityagina, G.B. Demishev, N.A. Bendeliani, Inorg. Chem. 39 (2003) 1198.
[15] C. Gong, Q.J. Li, R. Liu, Y. Hou, J.X. Wang, X.T. Dong, B. Liu, X. Yang, Z. Yao, X. Tan, D.M. Li, J. Liu, Z.Q. Chen, B. Zou, T. Cui, B.B. Liu, Phys. Chem. Chem. Phys. 15 (2013) 19925.
[16] Q. Li, S.R. Li, K. Wang, J. Liu, B.B. Liu, K. Yang, B. Zou, J. Phys. Chem. C 118 (2014) 7562.
[17] R.J. Curry, W.P. Gillin, Appl. Phys. Lett. 75 (1999) 1380.
[18] W.P. Gillin, R.J. Curry, Appl. Phys. Lett. 74 (1999) 798.
[19] H.K. Mao, J. Xu, P.M. Bell, J. Geophys. Res. 95 (1986) 4673.
[20] A.P. Hammersley, S.O. Svensson, M. Hanfland, A.N. Fitch, D. Häusermann, High Press. Res. 14 (1996) 235.
[21] K. Krämer, H. Romstedt, H.U. Güdel, P. Fischer, A. Murasik, M.T. Fernandez-Diaz, Eur. J. Solid State Inorg. Chem. 33 (1996) 273.

[22] A.C. Larson, R.B. Von Dreele, General Structure Analysis System, GSAS, Los Alamos National Laboratory Report LAUR , 1994, pp. 86–748.
[23] B.H. Toby, J. Appl. Cryst. 34 (2001) 210.
[24] F. Birch, Phys. Rev. 71 (1947) 809.
[25] F. Birch, J. Geophys. Res. 83 (1978) 1257.
[26] C. Gong, Structural Phase Transition and Photoluminescence Properties of Rare-Earth Fluoride under High Pressure Phd thesis, Jilin University, China, 2015.
[27] R. Reisfeld, G. Katz, C. Jacoboni, R. Depape, M.G. Drexhage, R.N. Brown, C. K. Jorgensen, J. Solid State Chem. 48 (1983) 323.
[28] M.D. Shinn, W.A. Sibley, M.G. Drexhage, R.N. Brown, Phys. Rev. B 27 (1983) 6635.
[29] M.J. Weber, T.E. Varitimos, B.H. Matsinger, Phys. Rev. B 8 (1973) 47.
[30] M.D. Wisser, M. Chea, Y. Lin, D.M. Wu, W.L. Mao, A. Salleo, J.A. Dionne, Nano Lett. 15 (2015) 1891.
[31] O.L. Malta, F.R.G. Silva, R. Longo, Chem. Phys. Lett. 307 (1999) 518.
[32] A. Nishikawa, N. Furukawa, T. Kawasaki, Y. Terai, Y. Fujiwara, Appl. Phys. Lett. 97 (2010) 051113.